

Alzheimer Diagnosis Method Based On Multi - Level Layers Approach

M AnanthaLakshmi, ECE, Assistant Professor,

Dr.A.Sanjeevi Kumar., M.E.,Ph.D, ECE, Assistant Professor

Abstract—Classical self-supervised networks suffer from convergence problems and reduced segmentation accuracy due to forceful termination. *Qubits* or bilevel quantum bits often describe quantum neural network models. In this article, a novel self-supervised shallow learning network model exploiting the sophisticated three-level *qutrit*-inspired quantum information system, referred to as quantum fully self-supervised neural network (QFS-Net), is presented for automated segmentation of brain magnetic resonance (MR) images. The QFS-Net model comprises a trinity of a layered structure of *qutrits* interconnected through parametric Hadamard gates using an eight-connected second order neighborhood-based topology. The nonlinear transformation of the *qutrit* states allows the underlying quantum neural network model to encode the quantum states, thereby enabling a faster self-organized counter propagation of these states between the layers without supervision. The suggested QFS-Net model is tailored and extensively validated on the Cancer Imaging Archive (TCIA) dataset collected from the Nature repository. The experimental results are also compared with state-of-the-art supervised (U-Net and URes-Net architectures) and the self-supervised QIS-Net model and its classical counterpart. Results shed promising segmented outcomes in detecting tumors in terms of dice similarity and accuracy with minimum human intervention and computational resources. The proposed QFS-Net is also investigated on natural gray-scale images from the Berkeley segmentation dataset and yields promising outcomes in segmentation, thereby demonstrating the robustness of the QFS-Net model.

Index Terms—Magnetic Resonance (MR) image segmentation, QIS-Net, quantum computing, *qutrit*, U-Net and URes-Net.

I. INTRODUCTION

QUANTUM computing supremacy may be achieved through the superposition of quantum states or quantum parallelism and quantum entanglement [1]. However, due to the lack of computing resources for the implementation of quantum algorithms, it is an uphill task to explore the quantum entanglement properties for optimized computation. Nowadays, with the advancement in quantum algorithms, the classical systems embedded in quantum formalism and inspired by *qubits* cannot exploit the full advantages of quantum superposition and quantum entanglement [2]–[4]. Due to the intrinsic characteristics offered by quantum mechanics, the implementation of quantum artificial neural networks (QANNs) has been proven to be successful in solving specific computing tasks, such as image classification and pattern recognition [5]–[8]. Nevertheless, quantum neural network models [9], [10] implemented on actual quantum processors are realized using a large number of quantum bits or *qubits* as matrix representation and linear operations on these vector matrices. However, due to complex and time-intensive quantum backpropagation algorithms involved in the supervised quantum-inspired artificial neural network (QINN) architectures [11], [12], the computational complexity increases manyfold with an increase in the number of neurons and interlayer interconnections.

Automatic segmentation of brain lesions from magnetic resonance imaging (MRI) greatly facilitates brain tumor identification overcoming the manual laborious tasks of human experts or radiologists [13]. It contrasts with the manual brain tumor diagnosis that suffers from significant variations in shape, size, orientation, intensity in homogeneity, overlapping of gray scales, and interobserver variability. Recent years have witnessed substantial attention in developing robust and efficient automated MR image segmentation procedures among the researchers of the computer vision community.

This work focuses on a novel quantum fully self-supervised neural network (QFS-Net) characterized by *qutrits* for fast and accurate segmentation of brain lesions. The primary aim of the suggested work is to enable the QFS-Net for faster convergence and making it suitable for fully automated brain lesion segmentation obviating any kind of training or supervision. The proposed QFS-Net model relies on *qutrits* or three-level quantum states to exploit the features of quantum correlation. To eliminate the complex quantum backpropagation algorithms used in the supervised QINN models, the QFS-Net resorts to a novel fully self-

supervised *qutrit*-based counter propagation algorithm. This algorithm allows the propagation of quantum states between the network layers iteratively. The primary contributions of this article are fourfold and are highlighted as follows.

- 1) Of late, the quantum neural network models and their implementation largely rely on *qubits*, and hence, we have proposed a novel *qudit* embedded generic quantum neural network model applicable for any level of quantum states, such as *qubit* and *qutrit*.
- 2) An adaptive multiclass quantum sigmoid (*QSig*) activation function embedded with quantum threat or *qutrit* is incorporated to address the wide variation of gray scales in MR images.
- 3) The convergence analysis of the QFS-Net model is provided, and its super linearity is also demonstrated experimentally.
- 4) The suggested QFS-Net model is validated extensively using the Cancer Imaging Archive (TCIA) dataset collected from Nature repository. Experimental results show the efficacy of the proposed QFS-Net model in terms of dice similarity, thus promoting self-supervised procedures for medical image segmentation. In addition to this, the proposed QFS-Net model is also investigated on natural gray-scale images from the Berkeley dataset to demonstrate its generalization on robust image segmentation.

The remaining sections of the article are organized as follows. Section reviews various supervised artificial neural networks and deep neural network models useful for brain MR image segmentation. A brief introduction of *qutrits* and generalized *D*-level quantum states (*qudits*) is provided along with the preliminaries of quantum computing. A novel quantum neural network model characterized by *qudits*. A vivid description of the suggested QFS-Net and its operations characterized by *qutrit* has been provided. Results and discussions shed light on the experimental outcome of the proposed neural network model. Concluding remarks and future directions of research are confabulated. In addition, the convergence analysis of the proposed network and quantum circuit design of QFS-Net for implementation on the actual quantum processor.

II. LITERATURE REVIEW

Recent years have witnessed various machine learning classifiers and deep learning technologies for automated brain lesion segmentation for tumor detection. Examples include U-Net and URes-Net, which have achieved remarkable dice score in auto segmentation of medical images. Of late, Pereira *et al.* suggested a modified convolutional neural network (CNN) introducing small-size kernels to obviate overfitting. Moreover, CNN-based architectures suffer due to a lack of manually segmented or annotated MR images, intensive preprocessing, and expert image analysts. In these circumstances, self-supervised or semi supervised medical image segmentation is becoming popular in the computer vision research community. Wang contributed an interactive method using deep learning with image-specific tuning for medical image segmentation. Zhuang *et al.* suggested Rubik's cube recovery-based self-supervised procedure for medical image segmentation. However, the interactive learning frameworks are not fully self-supervised and suffer from complex orientation and time-intensive operations.

QANNs were first proposed in the 1990s as a means of obviating some of the most recalcitrant problems that stand in the way of the implementation of large-scale quantum computing: algorithm design, noise and decoherence and scale up. Amalgamating artificial neural networks with the intrinsic properties of quantum computing enables the QANN models to evolve as promising alternatives to quantum algorithmic computing. Recent advances in both hardware and theoretical development may enable their implementation on the noisy intermediate-scale quantum (NISQ) computers that will soon be available. Konar *et al.* [7], [8], Behrman *et al.* Nguyen *et al.* Schütz hold and Masuyama *et al.* suggested quantum neural networks for pattern recognition tasks that deserve special mention for their contributions in this direction.

The classical self-supervised neural network architectures employed for binary image segmentation suffer from slow convergence problems. To overcome these challenges, the authors proposed the quantum version of the classical self-supervised neural network architecture relying on *qubits* for faster convergence and accurate image segmentation and implemented on classical systems [6]–[8]. Furthermore, the recently modified versions of the network architectures relying on *qubits* and characterized by multilevel activation function are also validated on MR images for brain lesion segmentation and reported promising outcome compared to the current deep learning architectures. However, the implementation of these quantum neural network models on classical systems is centered on the bilevel abstraction of *qubits*. In most physical implementations, the quantum states are not inherently binary thus, the *qubit* model is only an approximation that suppresses higher level states. The *qubit* model can lead to slow and untimely convergence and distorted outcomes. Here, three-level quantum states or *qutrits* (generally, *D*-level *qudits*) are introduced to improve the convergence of the self-supervised quantum neural network models.

A. Motivation

Despite the huge success of the deep learning-based neural networks for brain tumor segmentation the motivations behind

the proposed QFS-Net are given as follows.

- 1) Huge volumes of annotated medical images are required for suitable training of a CNN, which is, by itself, a paramount task.
- 2) The extensive and time-consuming training of deep neural network-based MR image segmentation requires high computational capabilities (GPU) and memory resources.
- 3) In contrast to automatic brain lesion segmentation, the slow convergence and overfitting problems often affect the outcome, and hence, extra efforts are required for suitable tuning of the hyperparameters of the underlying deep neural network architectures.
- 4) Moreover, the lack of image-specific adaptability of the CNNs leads to a fall in accuracy for unknown medical image classes.

A potential solution to circumvent the requirement of training data and the problems faced by the intensely supervised CNNs prevalent in medical image segmentation is a fully self-supervised neural network architecture with minimum human intervention. The novel qutrit-inspired fully self-supervised quantum learning model incorporated in the QFS-Net architecture presented in this article is a formidable contribution in exploiting the information of the brain lesions and poses a new horizon of research and challenges.

III. FUNDAMENTALS OF QUANTUM COMPUTING

Quantum computing offers the inherent features of superposition, coherence, decoherence, and entanglement of quantum mechanics in computational devices and enables the implementation of quantum computing algorithms. Physical hardware in classical systems uses binary logic; however, most quantum systems have multiple (D) possible levels. The states of these systems are referred to as *qudits*.

A. Concept of Qudits

In contrast to a two-state quantum system, described by a qubit, a ($D > 2$) multilevel quantum system is represented by D basis states

A general pure state of the system is a superposition of these basis states. We define generalized Pauli operators on *qudits* as $D-1$

where D th complex root of unity, i.e., the operator X shifts a computational basis state $|k\rangle$ to the next state, and the Z operator multiplies a computational basis state by the appropriate phase factor. Note that these two operators generate the generalized Pauli group.

The Hadamard gate is one of the basic constituents of quantum algorithms, as it creates a superposition of the basis states. On *qudits*, it is defined as subject to the normalization criterion $\sum_{i=0}^{D-1} |a_i|^2 = 1$, where. Physically, the absolute magnitude squared of a_0, a_1, \dots, a_{D-1} are complex quantities, $|a_0|^2 + |a_1|^2 + \dots + |a_{D-1}|^2 = 1$ each coefficient. i.e., $\{a_i\}$ represents the probability of the system being measured to be in the corresponding basis state $|i\rangle$.

In this article, we use a three-level system ($D = 3$), i.e., a basis of $\{|0\rangle, |1\rangle, \text{ and } |2\rangle\}$ qutrit for each quantum trit or is a spin-1 particle. A general *qutrit*. One physical example of a pure (coherent) state of a *qutrit* [40] is a superposition of all the three basis states, which can be represented as

$$|\psi\rangle = \alpha_0|0\rangle + \alpha_1|1\rangle + \alpha_2|2\rangle \quad \sum_{i=0}^2 |\alpha_i|^2 = 1 \quad (1)$$

subject to the normalization criterion $|\alpha_0|^2 + |\alpha_1|^2 + |\alpha_2|^2 = 1$.

The special case of the generalized Hadamard gate

We define a rotation gate in state has a probability of being measured to be in the basis state

Note that the rotation gate defined above is a unitary operator.

Similarly, the probabilities of the quantum state $(4/10)$ and $(3/10)$, respectively. $|\psi\rangle$ of being $|0\rangle$ and measured to be in each of the other two basis states $|1\rangle$ are:

a) QUANTUM NEURAL NETWORK MODEL BASED ON QUDITS (QNNM)

A quantum neural network dealing with discrete data is realized on a classical system using quantum algorithms and acts on quantum states through a layered architecture. In this proposed *qudit* embedded quantum neural network model theory the classical network inputs are converted into D -dimensional quantum states $[0, (2\pi/D)]$ or *qudits*. Let the k th input be given by

x_k .

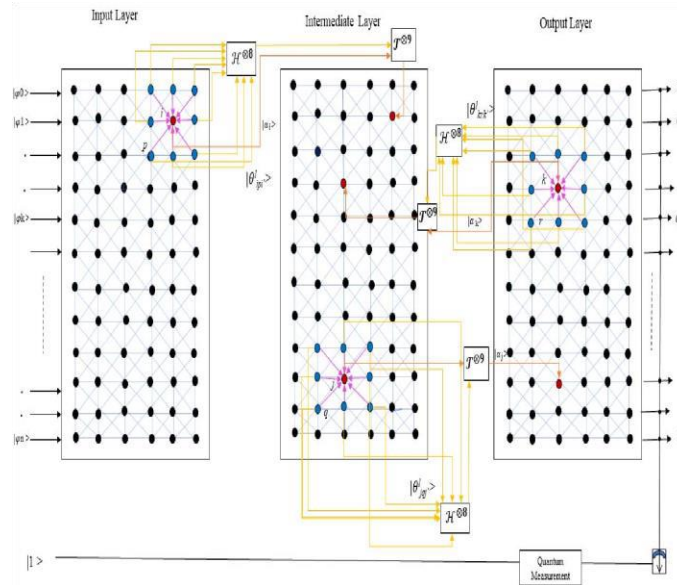


Fig: 1 Quantum Neural Networks

IV. QUANTUM FULLY SELF-SUPERVISED NEURAL NETWORK

The suggested QFS-Net architecture comprises trinity layers of *qutrit* neurons arranged as input, intermediate, and output layers. A schematic outline of the QFS-Net architecture as a quantum neural network model is illustrated in Fig. 1. The information processing unit of the QFS-Net architecture is depicted using quantum neurons (*qutrits*) reflected in the trinity layers using the combined matrix notation

Hence, each quantum neuron constitutes a *qutrit* state designated as ψ_{ij} . Each layer of the quantum self-supervised neural network architecture is organized by combining the *qutrit* neurons in a fully connected fashion with intra connection strength of $(2\pi/3)$ (*qutrit* state). The main characteristic of the network architecture lies in the organization of the eight connected second-order neighborhood subsets of each quantum neuron in the layers of the underlying architecture and propagation to the subsequent layers for further processing. The input, intermediate/hidden, and output layers are interconnected through self-forward propagation of the *qutrit* states in the eight-connected neighborhood fashion. On the contrary, the interconnections are established from the output layer to the intermediate layer entailing self-counter propagation obviating.

A. *Qutrit-Inspired Fully Self-Supervised Quantum Neural Network theory of each layer are realized using*

A connection weights are mapped using the phase Hadamard T transformation gate (realization mapping), and the inter-gates (H) applicable on *qutrits*. The angle of rotation is set to the relative difference of quantum fuzzy information (marked by pink arrow in Fig. 1 between each candidate *qutrit* neuron and the neighborhood *qutrit* neuron of the same layer employed in the rotation gate for updating the interlayer interconnections. The rotation angle for the interconnection for clarity weights and the threshold are set to ω and γ , respectively. The interconnection weights between the *qutrit* neurons (denoted as k and i) of two adjacent layers are depicted as $|\theta_{ik}\rangle$ and are measured as the relative difference between the candidate *qutrit* neuron and the eight-connected neighborhood quantum neuron k . The realization of the network weights is mapped using the Hadamard gate (model by suppressing the highest basic level (H) inspired by the proposed QNNM[2] of *qutrit* as a temporary storage.

The role of the relative measure of the quantum fuzzy information lies in the fact that the distinction between the foreground and background image pixels is clearly visible on adapting the relative measures. Assuming the quantum fuzzy grade information at the i th candidate neuron and its eight-connected second-order neighborhood neuron as μ_i and $\mu_{i,k}$, respectively, the angle of the

Hadamard gate is determined as $\omega_{i,k} = 1 - \mu_i - \mu_{i,k}; k \in \{1, 2, \dots, 8\}$.

The eight fully intra connected spatially arranged neighborhood *qutrit* neurons contribute to the candidate quantum neuron (say i) of the adjacent layer through the transformation gate (T) and the realization mapping defined as $|\psi_i\rangle = k T |\mu_{i,k}\rangle \mathcal{H}(\theta_{ik})$

In addition, the contributions of the eight fully intra connected spatially arranged neighborhood *qutrit* neurons are accumulated at the candidate *qutrit* neuron as the quantum fuzzy context-sensitive activation (ζ_i) and are presented using the Hadamard

gate as self-supervised quantum backpropagation algorithm, thereby reducing time complexity. Finally, a quantum observation process allows the *qutrit* states to collapse to one of the basis states (0 or 1 as 2 is considered as a temporary state). We obtain the true outcome at the output layer of the QFS-Net once the network converges; else, the quantum states = $Q\text{Sig} \quad q \quad 13 \times Q\text{Sig}$ the sum of the containment of eight-connected neighborhood *qutrit* neurons representing gray-scale pixels is denoted by $Q \quad N$. The generalized version of the $Q\text{Sig}$ activation function classical input to the neighborhood neuron p with respect to a candidate neuron i at the input layer, which is subsequently transformed to a *qutrit* state ($|\varphi\rangle = (2\pi/3)xip$), and is an imaginary unit. An adaptive multiclass *qutrit* embedded sigmoid ($Q\text{Sig}$) activation function employed in this self-supervised network model governs the activation at the intermediate and output layers and also the subsequent processing of the quantum states guided by various thresholding schemes.

B. Adaptive Multiclass Quantum Sigmoid Activation Function

In this article, we have introduced an adaptive multiclass sigmoid activation function in quantum formalism suitable for pixelwise multiclass segmentation of medical images varying with multi-intensity gray scales. The proposed $Q\text{Sig}$ activation function is the modification on the recently developed quantum multilevel sigmoid (QMSig) activation function employed in authors' previous work. An optimized version of a similar function. However, the requirement of finding optimal thresholds in images by the activation function is computationally exhaustive and time dependent. The proposed $Q\text{Sig}$ relies on an adaptive step length incorporating the total number of segmentation levels with various schemes of activation. The $Q\text{Sig}$ activation function, employed in the QFS-Net model, is defined as

$$Q\text{Sig}(x) = \frac{1}{\kappa\vartheta + e^{-\lambda(xh-\eta)}} \tag{2}$$

where $Q\text{Sig}(x)$ represents the adaptive multiclass $Q\text{Sig}$ activation function with a steepness parameter λ , a step size h , and an activation η described by *qutrits*. The multilevel class output, $\kappa\vartheta$ as *qutrit*, is defined as (c) $L = 6$. (d) subnormal responses σ $\kappa\vartheta$ as *qutrit*, where $0 \leq \kappa\vartheta \leq (2\pi/3)$. The multilevel class output is obtained on superposition of the subnormal.

V. RESULTS AND DISCUSSION

A. Dataset

Experiments have been performed on the TCIA dataset available from the Nature repository using the suggested QFS-Net model characterized by *qutrits* and an adaptive multiclass $Q\text{Sig}$ activation function. In contrast with the automatic brain lesion segmentation, four distinct activation schemes have been tested, and experiments are also performed using QFS-Net with QMSig activation function quantum inspired self-supervised network (QIS-Net) and its classical counterpart referred to as bidirectional self-organizing neural network (BDSONN) with multilevel sigmoid (MUSIG) activation function, and U-Net and URes-Net architectures. The U-Net and URes-Net architectures are trained with 2000 MR images and validated and tested on 120 and 880 contrast-enhanced dynamic susceptibility contrast (DSC) MR images, respectively. The proposed $Q\text{Sig}$ activation function is the modification on the recently developed quantum multilevel sigmoid (QMSig) activation function employed in authors' previous work

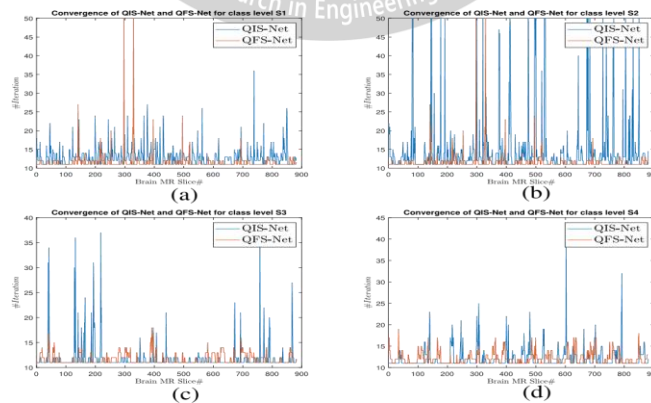


Fig:2 The gray-scale intensity index is expressed as L , where ϑ is the class index. The ϑ th and $(\kappa\vartheta - 1)$ th class responses are denoted by $\tau\vartheta$ and $\tau\vartheta - 1$, respectively,

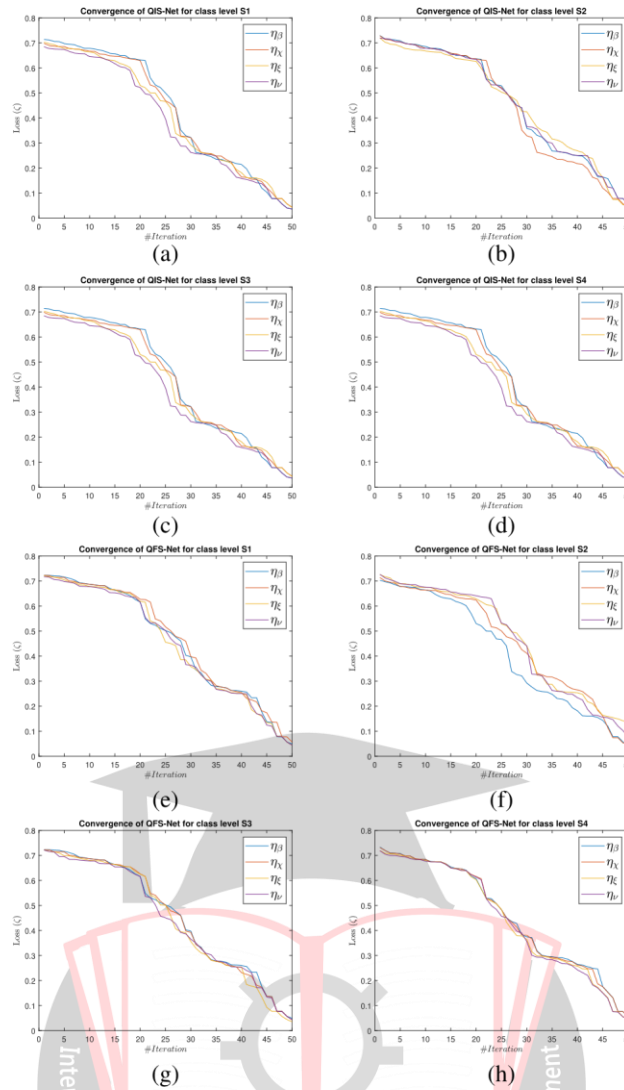


Fig. 3. Convergence analyses of the suggested *qutrit*-inspired QFS-Net and *qubits* embedded QIS-Net for four different activation schemes using gray-scale class levels S_1 , S_2 , S_3 , and S_4 (details are available in the Supplementary Material). (a) QIS-Net S_1 . (b) QIS-Net S_2 . (c) QIS-Net S_3 . (d) QIS-Net S_4 . (e) QFS-Net S_1 . (f) QFS-Net S_2 . (g) QFS-Net S_3 . (h) QFS-Net S_4 .

the same number of 880 contrast-enhanced DSC MR images. In addition to this, the proposed QFS-Net, QFS-Net with QMSig, and QIS-Net and its classical counterpart BDSONN with MUSIG are also investigated on natural gray-scale images from the Berkeley segmentation dataset.

B. Experimental Setup

In this work, extensive experiments have been carried out on 3000 DSC brain MR images of Glioma patients from the TCIA datasets of size 512×512 using a high-performance Nvidia RTX 2070 GPU System with MATLAB 2020a and Python 3.6. The 2-D segmented images are processed through a 2-D binary circular mask to obtain the brain lesion in the suggested QFS-Net framework. The lesion or brain tumor detection mask is binarized using a threshold of 0.5, and in the case of the proposed QFS-Net, QFS-Net with QMSig.

Experiments are also performed on two recently developed CNN architectures suitable for medical image segmentation, namely, convolutional U-Net and Residual U-Net (URes-Net) available in GitHub. The U-Net and URes-Net networks are rigorously trained using the stochastic gradient descent algorithm with a learning rate of 0.001 and a batch size of 32 allowing maximum of 50 epochs to converge. The segmented output images resemble in size with the dimensions of the binary mask, and the outcome 1 is considered as tumor region and 0 as background in detecting complete tumor. The pixel by pixel comparison with the manually segmented regions of interest (ROIs) or lesion mask allows evaluating the dice similarity, which is considered as a standard evaluation procedure in automatic medical image segmentation. The evaluation process involves the manually segmented lesion mask as ground truth, and each 2-D pixel is predicted as either true positive (TRP) or true negative (TRN) or false positive (FP) or false negative (FN).

The suggested *qutrit*-inspired fully self-supervised shallow quantum learning model, QFS-Net with QMSig and QISNet and its classical counterpart are experimented with the multilevel gray-scale images using distinct classes $L = 4, 5, 6, 7$, and 8 characterized by an adaptive multiclass QSig activation function. In this experiment, the steepness in the QSig activation in QFS-Net, λ , is varied in the range 0.23–0.24 with a step size of 0.001. It has been observed that, in the majority of cases, $\lambda = 0.239$ yields optimal performance. The empirical goodness measures (positive predictive value (PPV), sensitivity (SS), accuracy (ACC), and dice similarity (DS)) are assessed to evaluate the experimental outcome using four thresholding schemes ($\eta\beta, \eta\chi, \eta\zeta$, and $\eta\nu$), as discussed in the Supplementary Material, for different level sets. The dice score is often used to measure the similarity of the segmented brain lesions and ROIs. In addition to: The human expert segmented skull-tripped contrast-enhanced DSC brain MR input image slices of size 512×512 and ROIs are provided in Fig. 5 as samples.

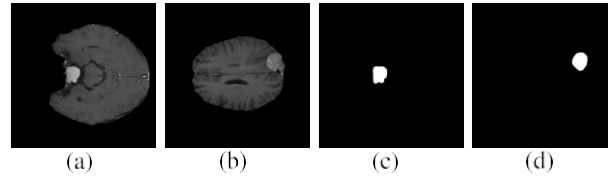


Fig. 4. DSC skull stripped brain MR images with size 512×512 and manually segmented ROI slices. (a) Input slice #37. (b) Input slice #69. (c) ROI slice #37. (d) ROI slice #69. images followed by the essential postprocessed outcome on slice no. 37 for class level $L = 8$ with four distinct activation schemes ($\eta\beta, \eta\chi, \eta\zeta$, and $\eta\nu$) is shown in Fig.6. It is evident from the experimental data.

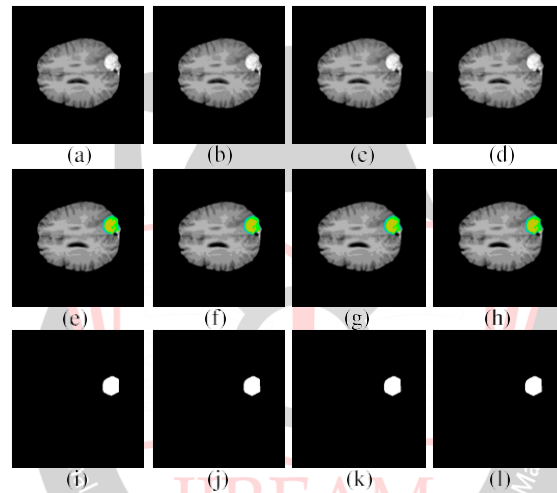


Fig. 5 Demonstration of QFS-Net segmented images followed by essential postprocessed outcome on the slice no. 37 [14] for class level $L = 8$ with four distinct activation schemes [(a), (e), (i), and (m) $\eta\beta$, (b), (f), (j), and (n) $\eta\chi$, (c), (g), (k), and (o) $\eta\zeta$, and (d), (h), (l), and (p) $\eta\nu$] with class levels for (a)–(d) $S1$, (e)–(h) $S2$, (i)–(l) $S3$, and (m)–(p) $S4$ [37].

C. Experimental Results

Extensive experiments have been performed in the current setup for brain MR image segmentation, and the experimental outcome is reported with the demonstration of numerical and statistical analyses using the proposed QFS-Net, QIS-Net, convolutional U-Net, and URes-Net architectures. The same number of 880 contrast-enhanced DSC MR images. In addition to this, the proposed QFS-Net, QFS-Net with QMSig, and QIS-Net and its classical counterpart BDSONN with MUSIG are also investigated on natural gray-scale images from the Berkeley segmentation dataset. The human expert segmented skull-tripped contrast-enhanced DSC brain MR input image slices of size 512×512 and ROIs are provided in Fig. 5 as samples. The demonstration of QFS-Net segmented.

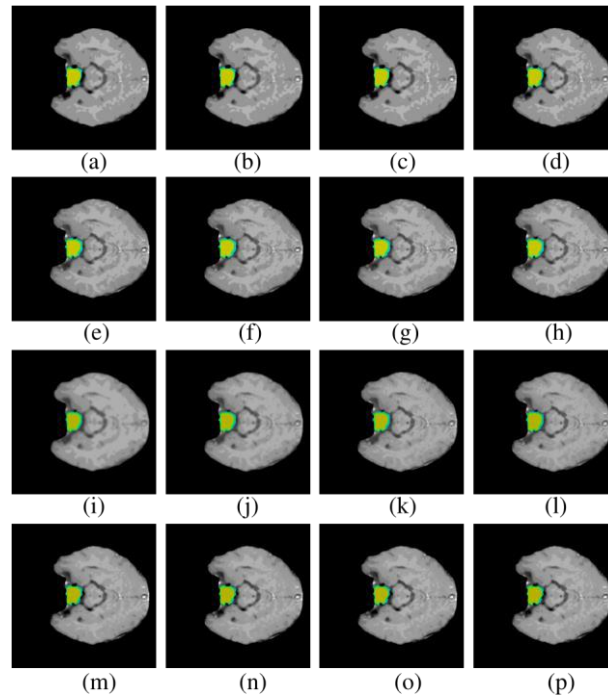


Fig. 6 Segmented ROIs describing the complete tumor region after the postprocessing using the proposed QFS-Net on slice #69 [14] using $L=8$ transition levels with four different thresholding schemes [(a), (e), and (i) $\eta\beta$, (b), (f), and (j) $\eta\chi$, (c), (g), and (k) $\eta\zeta$, and (d), (h), and (l) $\eta\nu$](a)–(e) with class-level $S1$. Segmented ROIs describing the complete tumor region after the postprocessing using the proposed QFS-Net on slice #69 [14] using $L=8$ Transition levels with four different thresholding schemes [(a), (e), and (i) $\eta\beta$, (b), (f), and (j) $\eta\chi$, (c), (g), and (k) $\eta\zeta$, and (d), (h), and (l) $\eta\nu$](a)–(e) with class-level $S2$. In this experimental setup, $\lambda=0.232$ yields optimal performance in terms of dice similarity (DS). The proposed *qutrit*-based quantum neural network model tries to explore the superposition and entanglement properties of quantum computing in classical simulations resulting in faster convergence of the network architecture, thereby yielding optimal segmentation.

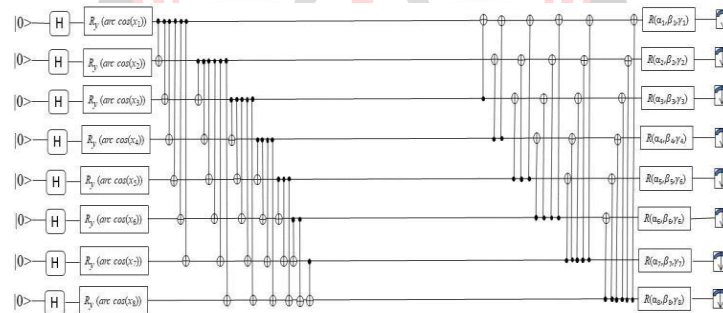


Fig.7 Generic VQC circuit of QFS-Net architecture where H and R_y represent a Hadamard gate and rotation about the Y -axis, respectively. Each VQC comprises data encoding layer, variational layer, and quantum measurement layer.

VI. CONCLUSION

The Counter part BDSONN with MUSIG. The box plots are also demonstrated in a section in the Supplementary Material citing the outcome reported in Tables II and III, respectively. Moreover, to show the effectiveness of our proposed QFS-Net over QFS-Net with QMSig, QIS-Net, BDSONN with MUSIG, U-net, and URes-Net, we have conducted a one-sided two sample Kolmogorov–Smirnov (KS) test with significance level $\alpha=0.05$. It is interesting to note that, in spite of being a fully self-supervised quantum learning model inspired by *qutrits*, QFS-Net has shown similar accuracy (ACC) and dice similarity (DS) compared with U-Net and URes-Net. Hence, it can be concluded that the performance of the QFS-Net model on brain MR images is statistically significant and offers a potential alternative to the solution of deep learning technologies.

In contrast to natural gray-scale image segmentation, the proposed QFS-Net segmented images are shown in Fig. 10 with the input gray-scale images from the Berkeley segmentation dataset. QFS-Net with QMSig, QIS-Net based on *qubits*, and BDSONN with MUSIG segmented images are shown in the Supplementary Material. The experimental results reported in Table IV indicate that the proposed QFS-Net outperforms all the other quantum-inspired self-supervised networks and the classical counterpart in terms of dice score compared with the human segmented images.

An automated brain tumor segmentation using a fully self supervised QFS-Net encompassing a qutrit-inspired quantum neural network model is presented in this work. The pixel intensities and interconnection weight matrix are expressed in quantum formalism on classical simulations, thereby reducing the computational overhead and enabling faster convergence of the network states. This intrinsic property of the QFS-Net model allows attaining accurate and time-efficient segmentation in real time. The suggested QFS-Net achieves high accuracy and dice similarity in spite of being a fully self supervised neural network model. Moreover, the proposed QFS-Net is investigated on natural gray-scale images, thereby demonstrating the robustness of the model.

The proposed quantum neural network model approach is also a faithful mapping toward quantum hardware circuit, and it can also be implemented on actual quantum processors using hybrid quantum-classical algorithms.

ACKNOWLEDGEMENT

In contrast to natural gray-scale image segmentation, the proposed QFS-Net segmented images with the input gray-scale images from the Berkeley segmentation dataset. QFS-Net with QMSig, QIS-Net based on qubits, and BDSONN with MUSIG segmented images are shown in the Supplementary Material. The experimental results reported in Table IV indicate that the proposed QFS-Net outperforms all the other quantum-inspired self supervised networks and the classical counterpart in terms of dice score compared with the human segmented images.

REFERENCES

- [1] V. Gandhi, Feb. 2014 G. Prasad, D. Coyle, L. Behera, and T. M. McGinnity, "Quantum neural network-based EEG filtering for a brain-computer interface," *IEEE Trans. Neural Netw. Learn. Syst.*, vol. 25, no. 2, pp. 278–288.
- [2] C. Chen, May 2014. D. Dong, H.-X. Li, J. Chu, and T.-J. Tarn, "Fidelity-based probabilistic Q-learning for control of quantum systems," *IEEE Trans. Neural Netw. Learn. Syst.*, vol. 25, no. 5, pp. 920–933.
- [3] P. Li Oct. 2013., H. Xiao, F. Shang, X. Tong, X. Li, and M. Cao, "A hybrid quantum-inspired neural networks with sequence inputs," *Neurocomputing*, vol. 117, pp. 81–90.
- [4] T.-C. Lu Aug. 2013. G.-R. Yu, and J.-C. Juang, "Quantum-based algorithm for optimizing artificial neural networks," *IEEE Trans. Neural Netw. Learn. Syst.*, vol. 24, no. 8, pp. 1266–1278.
- [5] S. Bhattacharyya, Nov. 2014. P. Pal, and S. Bhowmick, "Binary image denoising using a quantum multilayer self organizing neural network," *Appl. Soft Comput.*, vol. 24, pp. 717–729.
- [6] D. Konar, Sep. 2016. S. Bhattacharyya, B. K. Panigrahi, and K. Nakamatsu, "A quantum bi-directional self-organizing neural network (QBDSO) architecture for binary object extraction from a noisy perspective," *Appl. Soft Comput.*, vol. 46, pp. 731–752.
- [7] D. Konar, Sep. 2016, pp. 1912–1918. U. K. Chakraborty, S. Bhattacharyya, T. K. Gandhi, and B. K. Panigrahi, "A quantum parallel bi-directional self-organizing neural network (QBDSO) architecture for extraction of pure color objects from noisy background," in *Proc. Int. Conf. Adv. Comput., Commun. Informat. (ICACCI)*.
- [8] M. Schuld, Nov. 2014. I. Sinayskiy, and F. Petruccione, "The quest for a quantum neural network," *Quantum Information Process.*, vol. 13, pp. 2567–2586.
- [9] A. Kapoor, June 2017 N. Wiebe, and K. Svore, "Quantum perceptron models," in *Proc. Adv. Neural Inf. Process. Syst. (NIPS)*, vol. 29, 2016, pp. 3999–4007.
- [10] A. Narayanan and T. Menneer, Oct. 2000. "Quantum artificial neural network architectures and components," *Inf. Sci.*, vol. 128, nos. 3–4, pp. 231–255.
- [11] C. Y. Liu, Sep. 2013. C. Chen, C. T. Chang, and L. M. Shih, "Single-hidden-layer feed-forward quantum neural network based on Grover learning," *Neural Netw.*, vol. 45, pp. 144–150.
- [12] M. C. Clark, Apr. 1998. L. O. Hall, D. B. Goldgof, R. Velthuizen, F. R. Murtagh, and M. S. Silbiger, "Automatic tumor segmentation using knowledge based techniques," *IEEE Trans. Med. Imag.*, vol. 17, no. 2, pp. 187–201.
- [13] K. M. Schmainda, *Arch.*, 2016. M. A. Prah, J. M. Connelly, and S. D. Rand, "Glioma DSC-MRI perfusion data with standard imaging and ROIs [dataset]."